Design and Preparation of μ-Bimodal Porous Scaffold for Tissue Engineering

A. Salerno,[1,2] M. Oliviero,[3] E. Di Maio,[1] S. Iannace,[3] P. A. Netti[1,2]

[1]Interdisciplinary Research Centre in Biomaterials (CRIB), University of Naples Federico II, P.le Tecchio 80, 80125 Naples, Italy
[2]Italian Institute of Technology (IIT), Via Morego 30, 16163 Genoa, Italy
[3]Institute for Composite and Biomedical Materials (IMCB)-CNR, P.le Tecchio 80, 80125, Napoli, Italy

ABSTRACT: The aim of this study was to prepare poly-ε-caprolactone (PCL) foams, with a well-defined micrometric and bimodal open-pore dimension distribution, suitable as scaffolds for tissue engineering. The porous network pathway was designed without using toxic agents by combining gas foaming (GF) and selective polymer extraction techniques. PCL was melt-mixed with thermoplastic gelatin (TG) in concentrations ranging from 40 to 60 wt %, to achieve a cocontinuous blend morphology. The blends were subsequently gas foamed by using N_2-CO_2 mixtures, with N_2 amount ranging from 0 to 80 vol %. Foaming temperature was changed from 38 to 110°C and different pressure drop rates were used. After foaming, TG was removed by soaking in H_2O. The effect of blend compositions and GF process parameters on foam morphologies was investigated. Results showed that different combinations of TG weight ratios and GF parameters allowed the modulation of macroporosity fraction, microporosity dimension, and degree of interconnection. By optimizing the process parameters it was possible to tailor the morphologies of highly interconnected PCL scaffolds for tissue engineering. © 2007 Wiley Periodicals, Inc. J Appl Polym Sci 106: 3335–3342, 2007

Key words: scaffold; gas foaming; polymer extraction; macroporosity; microporosity

INTRODUCTION

One of the great challenges in tissue engineering is to design biocompatible and biodegradable scaffolds that provide the necessary support for cells to proliferate and maintain their differentiated function *in vitro* and/or *in vivo*, defining the ultimate shape of the new engineered tissue.[1]

Several techniques have been developed to prepare synthetic and natural polymeric scaffolds with a single scale porous network, including particulate leaching (PL),[2,3] gas foaming (GF),[4–6] and selective polymer extraction (PE) from cocontinuous blends.[7,8] Unfortunately, these methods showed great limitations in terms of scaffold design and function. For instance, scaffolds prepared via PL, by removing premixed percolated porogens from the polymeric matrix, possess a well-defined porosity and pore size. However, the presence of inorganic porogen particles eventually entrapped into the matrix may damage transplanted cells and represent a big limitation of this technique.[2] Furthermore, PL leads to a highly interconnected porosity with a drastic reduc-

tion of mechanical properties.[3] GF uses high-pressure gas processing to induce porosity formation into a polymeric matrix. The porosity and pore structure depend on the competition between gas bubble nucleation and growth and can be finely regulated by the selection of the blowing agent and processing parameters. However, this technique generally leads to scaffolds with partially closed cellular structure and nonporous external skin.[4] The PE technique involves the selective extraction of a polymeric phase from cocontinuous blends and provides scaffolds with mechanical properties suitable for load bearing application, such as bone and cartilage repair. In this case, scaffold porosity (ranging from 40 to 60% ca.), interconnectivity, and the difficulty in completely extracting the polymeric phase are the main limitations.[7,8]

Recently, advances in tissue engineering revealed that porosity architectures at different scales are key morphological properties of a scaffold to be used for the regeneration of complex three-dimensional tissues, such as bone and cartilage.[9] In particular, pores with mean diameters of the order of 100 μm (macroporosity) provide the necessary substrate for cells to adhere, grow, and proliferate. Furthermore, pores with diameters of few microns (microporosity), not accessible to cells but interconnected to the macroporosity, may represent a preferential way for fluids

Correspondence to: S. Iannace (iannace@unina.it).

and nutrients, providing the continuous supply for cell proliferation and biosynthesis and allowing the complete harvest of three-dimensional constructs.

With the aim of preparing scaffolds with a double-scale porosity (macroporosity and microporosity), thermally induced phase separation[10] or solvent casting (SC)/PL[11] techniques have been used recently. These process technologies, however, require the use of organics solvents that can remain in the scaffold, in turn damaging transplanted cells and biological signals eventually entrapped into the matrix.

To overcome this problem, GF/salt leaching (SL)[12,13] and PE/SL[14] methods have been applied to obtain porous networks on a double scale, with macroporosity formed after the removal of salt particles and microporosity created by GF or selective PE. If compared with SC/PL, these techniques allowed an increase of the exposure of bioactive particles on the scaffold surfaces and an increase of pores interconnectivity, with the consequence of enhancing bone regeneration efficacy of osteogenic cell transplantation for the treatment of bone defects.[13] The use of inorganic porogen and the difficulty of regulating the degree of interconnection by GF and selective PE represent to date the most important limitations for these techniques.

The aim of this study was to prepare poly-ϵ-caprolactone (PCL) scaffolds[15] with bimodal-micron scale porosity (μ-bimodal) without the use of toxic solvents and/or porogens, by combining the two techniques of GF and PE. This was achieved by: (i) preparing PCL and thermoplastic gelatin (TG) (a highly water-soluble natural polymer from animal protein) cocontinuous blends, (ii) GF the blends with physical blowing agent mixtures, and (iii) extracting the TG by submerging the foamed samples in water.

The correspondence between blend composition and cocontinuous blend morphologies and the effect of blend composition, foaming temperature, blowing agent, and pressure drop rate on foaming were studied to optimize macroporosity fraction, microporosity dimension, and degree of interconnection of the final PCL scaffolds.

EXPERIMENTAL

Materials

PCL ($M_W = 65$ kDa, $T_m = 59$–$64°C$, $T_g = -60°C$, and $\rho = 1.145$ g/cm^3) and gelatin powder (type B, $M_W = 40$–50 kDa) were purchased from Sigma–Aldrich (Italy). Glycerol anhydrous with purity grade higher than 99.5% was purchased from Fluka (Italy) and used as plasticizer for the preparation of TG. N_2 and CO_2 mixtures (Air liquide, Italy) were used as physical blowing agent for GF experiments.

TABLE I
Abbreviations and Weight Compositions of PCL/TG Blends

	PCL/TG$_{60/40}$	PCL/TG$_{55/45}$	PCL/TG$_{50/50}$	PCL/TG$_{40/60}$
PCL	60	55	50	40
TG	40	45	50	60

Blends preparation

Cocontinuous blends were prepared with PCL and thermoplasticized gelatin. Thermoplasticization is a thermomechanical process used to induce, with the aid of suitable plasticizers, the formation of a thermoplastic material out of the original hierarchical-structured natural polymers.[16] TG was prepared by using an internal mixer (Rheomix® 600 Haake, Germany) controlled by a measuring drive unit (Haake Rheocord® 9000). 50 g of gelatin powder were mixed with 20 wt % of glycerol at $60°C$, 60 rpm for 6 min. The TG was then extracted from the mixer and ground for further processing. Subsequently, PCL-TG blends were obtained with the same mixing equipment at $60°C$, 80 rpm for 6 min. PCL-TG composition, ranging from 60 to 40 to 40–60 wt % (see Table I), were chosen in the region of the inversion point[17,18] ($\rho_{TG} = 1.18$ g/cm^3, as evaluated by gravimetric and volumetric measurement). Finally, the blends were extracted from the mixer and compressed at $70°C$ and 30 bar into 2 mm-thick plates by a P 300 P hot press (Collin, Germany).

Achievement of the porous structures: GF and TG extraction

Physical batch foaming was conducted in a high-pressure vessel (HiP, US) as described by Marrazzo et al.,[19] adapted to provide a fine control of the basic foaming parameters: blowing mixture composition, foaming temperature (T_F), saturation pressure (P_{sat}), and pressure drop rate (PDR).[20–22]

Samples were solubilized with the blowing mixture for 4 h at $70°C$ and subsequently cooled or heated to the desired foaming temperatures with a precise protocol. The pressure was then released to ambient pressure with controlled pressure drop rates (PDRs). Three GF processing variables were selected to modulate foam morphologies: N_2-CO_2 blowing mixture (0–100 to 80–20 vol %), T_F in the range 38–$110°C$ and PDR from 70 to 700 bar/s. Foams were finally soaked at $38°C$ in distilled H_2O until complete TG extraction and subsequently dried to achieve the final scaffold architectures.

Morphological analysis

Scanning electron microscopy (SEM) and image analysis were used to assess foamed sample morphologies

and to determine the volume fraction of the single foamed components by means of the area fraction measurements.[23,24] Samples were cross-sectioned, gold sputtered, and analyzed by SEM LEICA S440 at an accelerating voltage of 20 kV, at various magnifications.

Image analysis [Image J[®]] was used as a numerical tool to evaluate the effect of blend compositions and GF process parameters on the multiphase morphology of the foams. In particular, the volume fraction of the expanded TG phase (Φ), defined as (eq. (1)):

$$\Phi = \frac{\text{volume of foamed TG phase}}{\text{total volume of foamed sample}}, \qquad (1)$$

was identified with the TG area fraction[23,24] and was measured by tracing the areas of foamed PCL and TG from a 7 mm^2 micrograph. The image magnification (90×) was chosen as a compromise between phase resolution and error related to the mean phase domain dimension. Moreover, the morphology of each phase was characterized by the average size of bubbles within the expanded PCL phase (D_{PCL}) and the expanded TG phase (D_{TG}). D_{PCL} and D_{TG} were evaluated from SEM micrographs by tracing a minimum of 150 pores for each phase and correcting the software value, calculated with the hypothesis of spherical shape, with the factor $4/\pi$, according to the ASTM D 3576.

By considering that the PCL microstructure is unvaried after the TG extraction, Φ corresponds to the macroporosity volume fraction and D_{PCL} corresponds to the microporosity characteristic dimension of the final PCL scaffolds.

RESULTS AND DISCUSSION

The architecture of the porous structure in our system strongly depends on several factors, related to the materials and the processes involved. In particular, the composition of the blend (PCL/TG), the kind of process (blending and foaming), and the composition of the blowing agent (N_2/CO_2) are the parameters that affect the final morphology.[25] Moreover, the analysis is further complicated since all of these parameters are mutually correlated and interdependent. For instance, blend composition is one of the most important parameters in defining cocontinuous morphologies and, hence, macroporosity of the final scaffolds. However, this parameter also affects PCL foaming and therefore scaffold microporosity. To make our analysis simpler, this study will be mostly devoted to the understanding of the GF process, once the effective cocontinuity and characteristic dimensions of the phases have been verified.

### Cocontinuous blends characterization

The achievement of heterogeneous blends was confirmed by dynamic mechanical thermal analysis, which showed the presence of the two T_g's of the single components (at $-60°C$ for PCL and $50°C$ for TG, consistently with DSC results[26]). Furthermore, the cocontinuous morphology patterns of the blends were verified by electron microscopy and gravimetric measurements after TG extraction. These results (not shown) confirmed the complete removal of the TG for all the PCL/TG blends.

Gas foaming of cocontinuous blends

The effect of blend composition and GF process parameters (T_F, blowing mixture composition, and PDR) on Φ, D_{PCL}, and D_{TG} in PCL/TG foamed blends was investigated, with the aim of modulating the volume fractions of the two phases and achieving open-celled PCL foams. As a co-effect, TG phase will also foam, but its porous structure is of minor importance since it will be subsequently removed.

Effect of blend composition on foam microstructures

SEM micrographs of the foams prepared from all the blends (see Table I) by using a 80–20 vol % N_2-CO_2 mixture as the blowing agent, at $T_F = 43°C$, $P_{sat} = 180$ bar, and PDR = 700 bar/s, are shown in Figure 1. The PCL/TG$_{60/40}$ and PCL/TG$_{40/60}$ systems [Fig. 1(a,d)] showed a morphology characterized by two foamed phases, while the PCL/TG$_{55/45}$ and PCL/TG$_{50/50}$ [Fig. 1(b,c)] systems showed a negligible expansion of the TG phase. The porosities of the two phases are rather different, with expanded TG phase characterized by smaller pores with respect to expanded PCL phase. Figure 2 reports the effect of TG concentration on Φ, D_{PCL}, and D_{TG}. As expected, Φ increases (from 0.2 to 0.65 ca.) with the increase of TG content in the original blend composition. In particular, at the lower TG concentrations (from 40 to 50 wt %), Φ was less than nominal TG concentration, showing a more pronounced expansion of the PCL phase. At the highest TG concentration (60 wt %), conversely, Φ = 0.65 demonstrated an increased expansion of the TG phase. D_{PCL} decreases progressively from 50 μm for the system PCL/TG$_{60/40}$ to 30 μm for the system PCL/TG$_{50/50}$ and increases with further increase of TG (50 μm for PCL/TG$_{40/60}$). When expanded (systems PCL/TG$_{60/40}$ and PCL/TG$_{40/60}$), the TG phase showed a foam morphology with D_{TG} between 10 and 20 μm. Taking into account these results, we selected the PCL/TG$_{60/40}$ system [Fig. 1(a)] for further GF investigations.
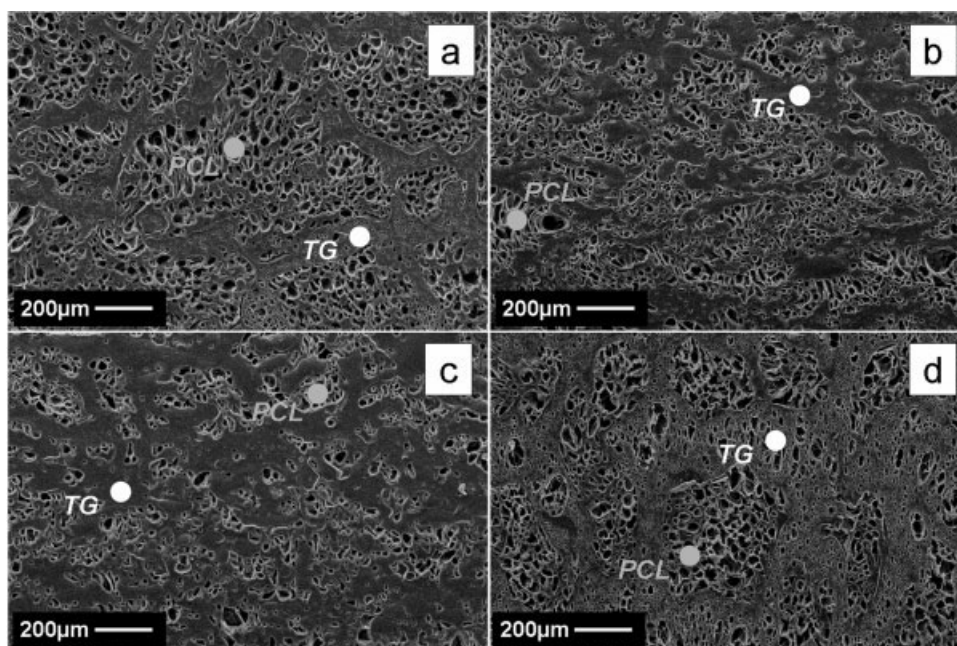
Figure 1 SEM micrographs of PCL/TG$_{60/40}$ (a), PCL/TG$_{55/45}$ (b), PCL/TG$_{50/50}$ (c), and PCL/TG$_{40/60}$ (d) blends foamed with 80–20 vol % N$_2$-CO$_2$ blowing mixture at T_F = 43°C, P_{sat} = 180 bar, and PDR = 700 bar/s.

Effect of foaming temperature on foam microstructures

Figure 3 shows SEM picture of PCL/TG$_{60/40}$ foam morphologies, prepared in the T_F range of 38–110°C, using a 80–20 vol % N$_2$-CO$_2$ mixture, at P_{sat} = 180 bar and PDR = 700 bar/s. Figure 3(a) shows that, at 38°C, TG did not foam at all. This effect is related to the glass transition temperature of TG (T_g = 50°C, see earlier section), which could be eventually lowered by the presence of blowing agent (plasticizing effect). In fact, at temperatures below the T_g of the TG/blowing agent solution, foaming is hindered by the very high rigidity of the glassy polymer, while at temperatures higher than or equal to 42°C, TG was able to expand, giving fine-celled morphologies. Regarding the PCL phase, the porous structures change drastically whether the T_F is lower or higher than the PCL melting temperature (T_m). In fact, at T_F higher than 60°C, PCL do not crystallize and the foamed structure collapsed. The resulting morphologies of the PCL/TG system are then characterized by a foamed TG phase surrounded by a collapsed, dense PCL phase [see Fig. 3(d)]. These effects are also described by the Φ, D_{PCL}, and D_{TG} versus T_F curves, reported in Figure 4. When $T_F < T_m$, Φ decreases with the increase of T_F up to 42°C, for the improved tendency of PCL to foam [Fig. 3(a,b)], and then increases, as a result of the increased tendency of PCL to collapse [Fig. 3(c)]. Finally, when $T_F > T_m$, Φ is almost constant and equals to 0.33. As already observed in the previous section, PCL foams give coarser porous structures with respect to TG. At

$T_F > T_m$, furthermore, D_{PCL} increased of almost one order of magnitude for the extensive bubble coalescence. The effect of the other processing parameters on foam microstructures was then studied by selecting T_F in the range 42–45°C.

Effect of blowing mixture composition on foam microstructures

The effect of the blowing agent composition on PCL/TG$_{60/40}$ was studied in the range 0–100 to 80–
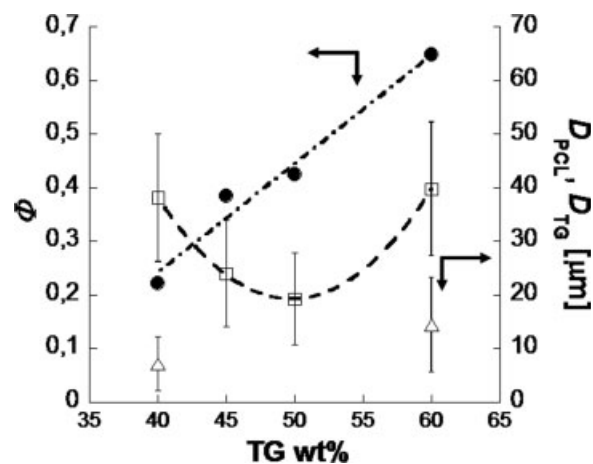

Figure 2 Effect of blend compositions on Φ (●), D_{PCL} (□), and D_{TG} (△) for samples prepared with 80–20 vol % N$_2$-CO$_2$ blowing mixture, T_F = 43°C, P_{sat} = 180 bar, and PDR = 700 bar/s. Black symbols refer to the left axis and closed symbols refer to the right axis.
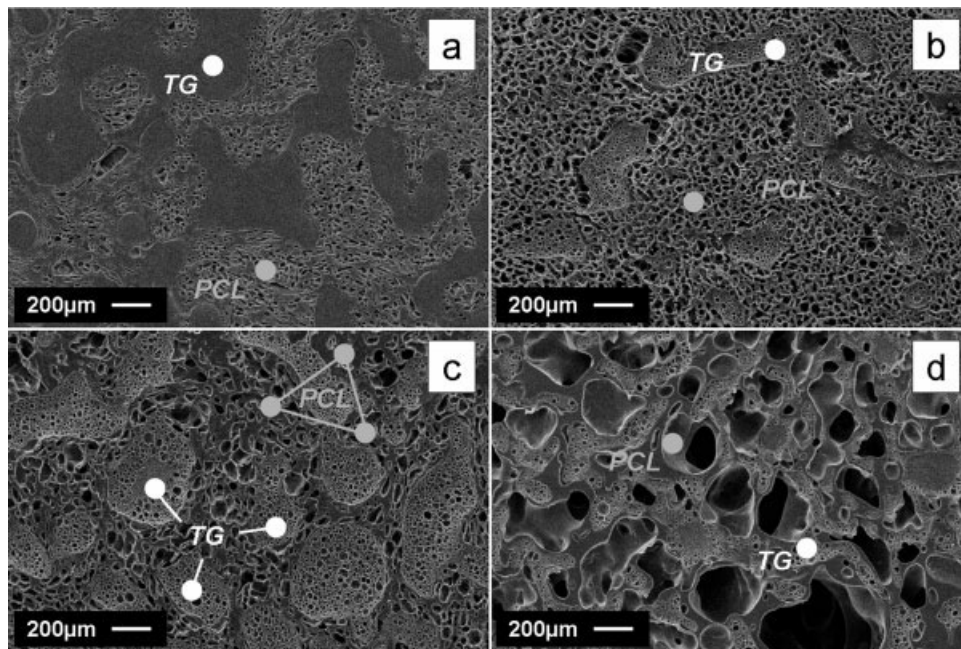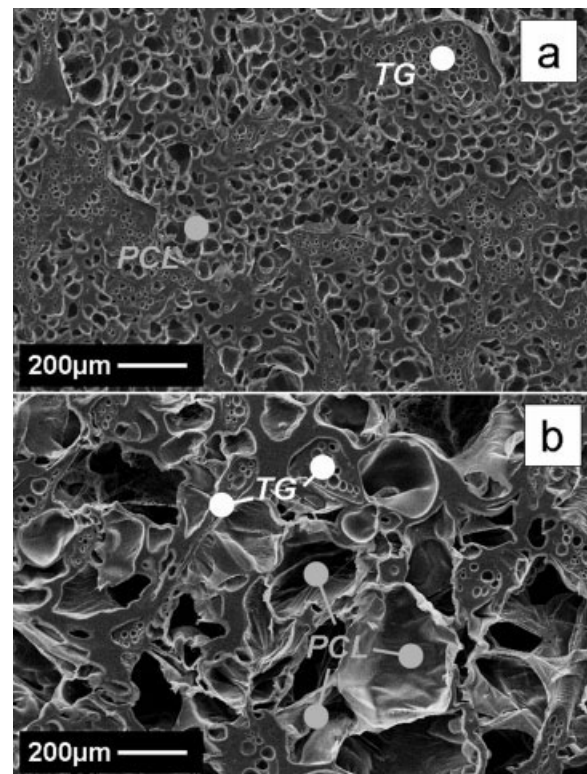
Figure 3 SEM micrographs of PCL/TG$_{60/40}$ blend foamed with 80–20 vol % N$_2$-CO$_2$ blowing mixture at different T_F: 38°C (a), 44°C (b), 50°C (c), and 70°C (d).

20 vol % N$_2$-CO$_2$, at T_F = 43°C. P_{sat} changed in the range 100 (for the 0–100 mixture) to 180 bar (80–20) and PDR changed accordingly, from 500 to 700 bar/s, respectively. SEM micrographs of selected foams are shown in Figure 5, while Φ, D_{PCL}, and D_{TG} curves are reported in Figure 6. Results show that the porous structure of the PCL/TG$_{60/40}$ samples is strongly affected by the gas mixture composition. In particular, in the range 80–20 to 50–50 vol %, foams were characterized by two foamed phases [Figs. 1(a), 3(b), and 5(a)], with finer TG phase morphologies with respect to the PCL phase. With further increase

of CO$_2$, the TG phase foams did not change significantly, while PCL foams were characterized by coarse and mainly closed-cell structures. The differences in the foaming behavior of the two different
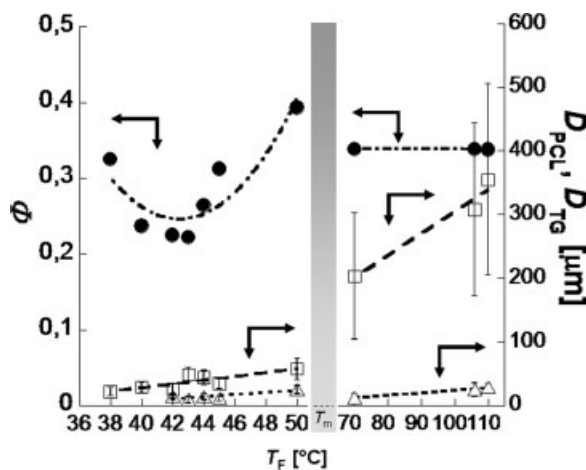
Figure 4 Effect of T_F on Φ (●), D_{PCL} (□), and D_{TG} (△) of PCL/TG$_{60/40}$ blend foamed with 80–20 vol % N$_2$-CO$_2$ blowing mixture, P_{sat} = 180 bar and PDR = 700 bar/s. Closed symbols refer to the left axis and open symbols refer to the right axis.

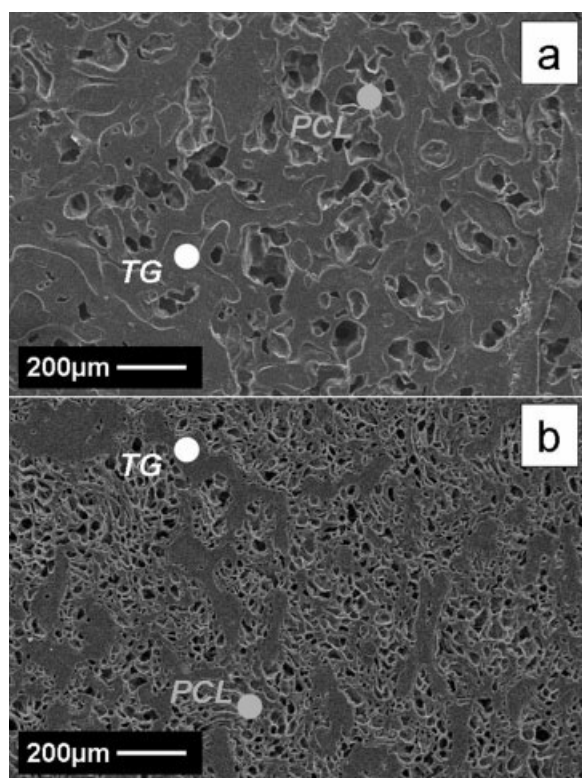**Figure 5** SEM micrographs of PCL/TG$_{60/40}$ blend foamed at T_F = 43°C with different CO$_2$-N$_2$ blowing mixture: (a) 40–60 vol %, (b) 70–30 vol %.
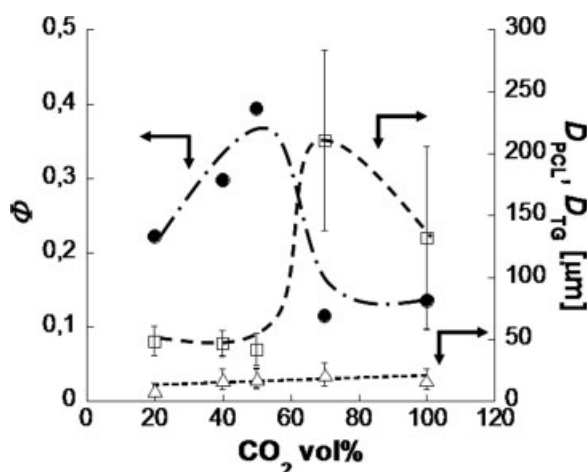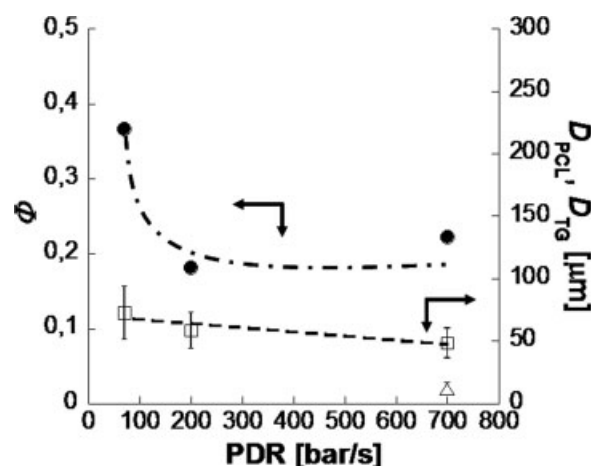
Figure 6 Effect of blowing mixture composition on Φ ($\bullet$), D_{PCL} ($\square$), and D_{TG} ($\triangle$) of PCL/TG$_{60/40}$ blend foamed with $T_F = 43°C$ and PDR = 700 bar/s. Closed symbols refer to the left axis and open symbols refer to the right axis.

Figure 8 Effect of PDR on Φ ($\bullet$), D_{PCL} ($\square$), and D_{TG} ($\triangle$) of PCL/TG$_{60/40}$ blend foamed with 80–20 vol % N_2-CO_2 blowing mixture at $T_F = 43°C$ and $P_{sat} = 180$ bar. Closed symbols refer to the left axis and open symbols refer to the right axis.

phases could be ascribed to the different solubilities and related plasticization effect of the blowing mixtures. In particular, with the increase of CO_2 content beyond 50 vol %, elongational properties of PCL dramatically decreased, resulting in the impossibility to withstand the elongational stresses during foaming. In fact, the increased plasticization effect of CO_2

Figure 7 SEM micrographs of PCL/TG$_{60/40}$ blend foamed with 80–20 vol % N_2-CO_2 blowing mixture at $T_F = 43°C$ and $P_{sat} = 180$ bar with different PDR: 70 bar/s (a) and 200 bar/s (b).

could be described as a temperature increase, which, as observed before, could lead to cell collapse. Conversely, TG did not present any collapse in the analyzed experimental range of blowing agent composition, as observed earlier, in the analysis of the effect of T_F [Fig. 5(b)], proving a wider foaming window with respect to PCL. The effect of PDR on foam microstructures was investigated by selecting 80–20 vol % N_2-CO_2 blowing mixture during next foaming experiments.

Effect of PDR on foam microstructures

The effect of PDR on PCL/TG$_{60/40}$ foam microstructures was evaluated in the range 70–700 bar/s, by GF with 80–20 vol % N_2-CO_2 mixture as the blowing agent, at $T_F = 43°C$ and $P_{sat} = 180$ bar. SEM micrographs of samples foamed at PDR of 70, 200, and 700 bar/s [Figs. 7(a,b) and 1(a) respectively] show morphologies characterized by PCL porous structure and limited expansion of the TG phase in the whole range of PDR. Φ and D_{PCL} decrease significantly from 70 to 700 bar/s, as shown in Figure 8.[22] We finally selected PDR = 700 bar/s to prepare the PCL scaffolds.

PCL scaffold preparation by TG extraction

Results of TG extraction are reported in Figures 9 and 10. Figure 9 shows SEM micrograph of the scaffold prepared at $T_F = 70°C$, by foaming PCL/TG$_{60/40}$ blend with 80–20 vol % N_2-CO_2 at $P_{sat} = 180$ bar and PDR = 700 bar/s. The morphology is characterized by a single-scale porous network with rounded and well interconnected macropores. In fact, when foaming process is achieved at $T_F > T_m$, PCL expands and soon collapses on the TG walls, as previously

described, thus creating macropores on the same dimension of the pores created by TG extraction.

SEM micrographs of the scaffold prepared at $T_F = 44°C$, by foaming PCL/TG$_{60/40}$ blend with 80–20 vol % N$_2$-CO$_2$ at $P_{sat} = 180$ bar and PDR = 700 bar/s, are reported in Figure 10. As expected, the lower magnification of Figure 10a reveals that by this technique it is possible to prepare scaffold with pore size and shape on a double scale: (i) macroporosity created by the removal of TG foamed phase and (ii) microporosity formed during PCL foaming. In particular, the macroporosity appears elongated, interconnected, and homogeneously distributed around open and circular shaped microporosity ($D \sim 30$ μm), as evidenced in Figure 10b. The micrograph of Figure 10c shows the morphology of the polymeric walls between macroporosity and microporosity. The image reveals that the macroporosity walls appear rough and porous, with an homogeneous distribution of circular pores ($D \sim 10$ μm). This third scaled porosity is probably originated by the rupture of PCL bubble walls at the interface with TG and led to the formation of a single and highly interconnected macro and micro-porous network, necessary for the growth of thick cross sections of tissue.[27–29]

CONCLUSIONS

The present study investigated the feasibility of preparing PCL scaffolds with a well controlled porous architecture without using toxic solvents and/or porogens. PCL and TG polymers and GF and PE techniques were selected and combined to regulate scaffold morphology on a single or double scale.

The effect of PCL/TG blend composition and GF process parameter (blowing mixture composition, PDR, and T_F) on foamed blend morphologies was studied to design the final scaffold architectures.
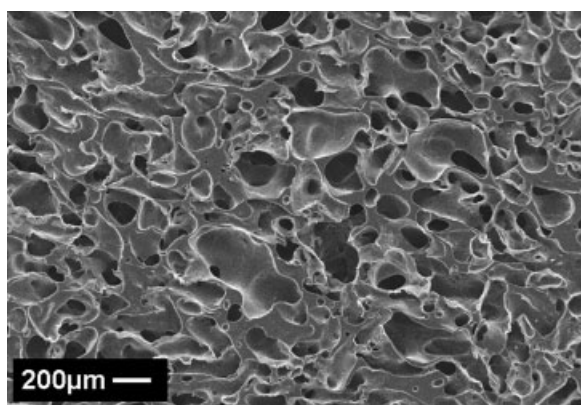
Figure 9 SEM micrograph of PCL scaffold prepared by GF/PE technique from PCL/TG$_{60/40}$ blend foamed with 80–20 vol % N$_2$-CO$_2$ blowing mixture, $P_{sat} = 180$ bar, PDR = 700 bar/s at $T_F = 70°C$.
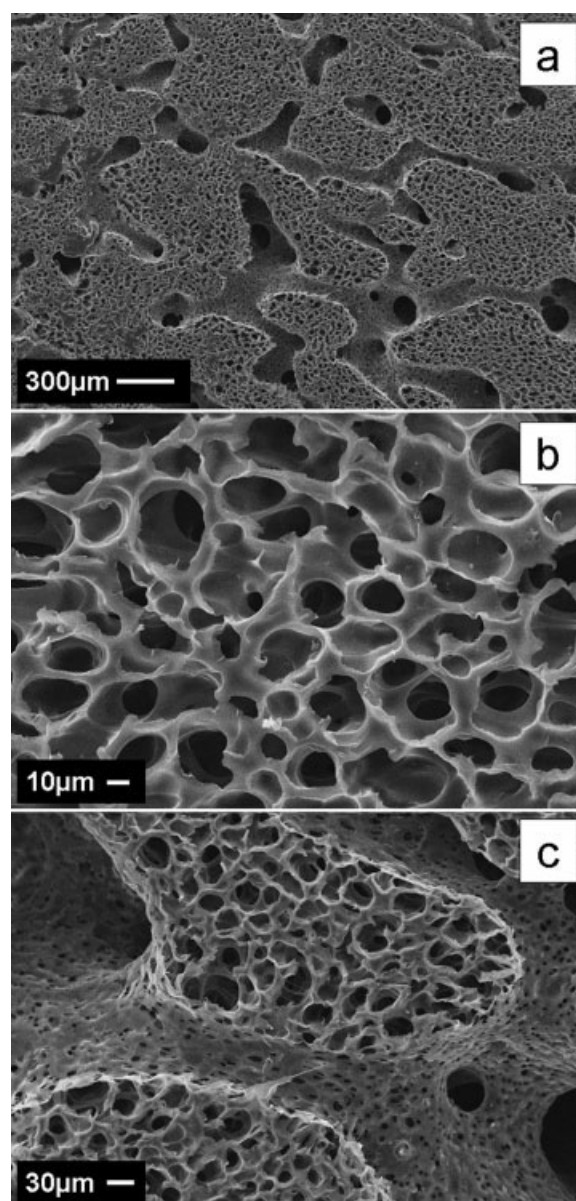
Figure 10 SEM micrographs of μ-bimodal PCL scaffold prepared by GF/PE technique from PCL/TG$_{60/40}$ blend foamed with 80–20 vol % N$_2$-CO$_2$ blowing mixture, $P_{sat} = 180$ bar, PDR = 700 bar/s at $T_F = 44°C$.

Scaffold with a single scale porous network was prepared from PCL/TG$_{60/40}$ blend by GF with 80–20 vol % N$_2$-CO$_2$ blowing mixture, $P_{sat} = 180$ bar, PDR = 700 bar/s, and $T_F = 70°C$.

μ-Bimodal and highly interconnected PCL scaffold with pore shape and dimension on a double scale was prepared by selecting $T_F = 44°C$ and unvarying the other process parameters.

These results suggest that the appropriate selection of blend composition and GF process parameters allows the design of highly interconnected porous network of PCL scaffolds suitable to be used for tissue engineering.

References

1. Hutmacher, D. W. Biomaterials 2000, 21, 2529.
2. Mikos, A. G.; Thorsen, A. J.; Czerwonka, L. A.; Bao, Y.; Langer, R.; Winslow, D. N.; Vacanti, J. P. Polymer 1994, 35, 1068.
3. Zhou, Q.; Gong, Y.; Gao, C. J Appl Polym Sci 2005, 98, 1373.
4. Mooney, D. J.; Baldwin, D. F.; Suh, N. P.; Vacanti, J. P.; Langer, R. Biomaterials 1996, 17, 1417.
5. Mathieu, L. M.; Mueller, T. L.; Bourban, P.; Piolettic, D. P.; Muller, R.; Manson, J. E. Biomaterials 2006, 27, 905.
6. Yang, X.; Tare, R. S.; Partridge, K. A.; Roach, H. I.; Clarke, N. M. P.; Howdle, S. M.; Shakesheff, K. M.; Oreffo, R. O. C. J Bone Min Res 2003, 18, 47.
7. Sarazin, P.; Roy, X.; Favis, B. D. Biomaterials 2004, 25, 5965.
8. Washburn, N. R.; Simon, C. G., Jr.; Tona, A.; Elgendy, H. M.; Karim, A.; Amis, E. J. J Biomed Mater Res 2002, 60, 20.
9. Karageorgiou, V.; Kaplan, D. Biomaterials 2005, 26, 5474.
10. Gong, Y.; Ma, Z.; Gao, C.; Wang, W.; Shen, J. J Appl Polym Sci 2006, 101, 3336.
11. Wei, G.; Ma, P. X. Biomaterials 2004, 25, 4749.
12. Harris, L. D.; Kim, B.; Mooney, D. J. J Biomed Mater Res 1998, 42, 396.
13. Kim, S.; Park, M. S.; Jeon, O.; Choi, C. Y.; Kim, B. Biomaterials 2006, 27, 1399.
14. Reignier, J.; Huneault, M. A. Polymer 2006, 47, 4703.
15. Hutmacher, D. W.; Schantz, T.; Zein, I.; Ng, K. W.; Teoh, S. H.; Tan, K. C. J Biomed Mater Res 2001, 55, 203.
16. Di Gioia, L.; Guilbert, S. J Agric Food Chem 1999, 47, 1254.
17. Willemse, R. C.; De Boer, A. P.; Van Dam, J.; Gotsis, A. D. Polymer 1998, 39, 5879.
18. Galloway, J. A.; Jeon, H. K.; Bell, J. R.; Macosko, C. W. Polymer 2005, 46, 183.
19. Marrazzo, C.; Di Maio, E.; Iannace, S.; Nicolais, L. J Cell Plast, to appear.
20. Klempner, D.; Frisch, K. C. Handbook of Polymeric Foams and Foam Technology. Hanser Gardener: New York, 1991.
21. Di Maio, E.; Mensitieri, G.; Iannace, S.; Nicolais, L.; Li, W.; Flumerfelt, R. W. Polym Eng Sci 2005, 45, 432.
22. Park, C. B.; Baldwin, D. F.; Suh, N. P. Polym Eng Sci 1995, 35, 432.
23. Whitaker, S. Ind Eng Chem 1969, 61, 14.
24. Kwak, K. D.; Okada, M.; Chiba, T.; Nose, T. Macromolecules 1992, 25, 7204.
25. Taki, K.; Nitta, K.; Kihara, S.; Ohshima, M. J Appl Polym Sci 2005, 97, 1899.
26. Salerno, A.; Oliviero, M.; Di Maio, E.; Iannace, S. Int Polym Proc, to appear.
27. Sachlos, E.; Czernuszka, J. T. Eur Cells Mater 2003, 5, 29.
28. Ishaug-Riley, S. L.; Crane, G. M.; Gurlek, A.; Miller, M. J.; Yasko, A. W.; Yaszemski, M. J.; Mikos, A. G. J Biomed Mater Res 1997, 36, 1.
29. Heslop, B. F.; Zeiss, I. M.; Nisbet, N. W. Br J Exp Path 1960, 41, 269.